



Chemical and Structural Characteristics of Biochars from Phytoremediation Biomass of *Cymbopogon Citratus*, *Cymbopogon Nardus*, and *Chrysopogon Zizanioides*

Katlarelo L. Sefatli¹ · Venecio U. Ultra Jr¹ · Stephen Majoni²

Received: 17 August 2022 / Accepted: 7 May 2023 / Published online: 19 May 2023
© The Author(s), under exclusive licence to Springer Nature B.V. 2023

Abstract

Purpose This study characterizes the chemical and structural properties of biochar derived from phytoremediation biomasses of *Cymbopogon citratus*, *Cymbopogon nardus*, and *Chrysopogon zizanioides*. This provide information on the conversion of phytoremediation biomass to biochar as a promising prospect to enhance biomass utilization and management in a phytoremediation system.

Research Question What are the effects of the heavy metal (HM) contents of biomass on the biochar's structural and chemical properties during pyrolysis?

Methods The three types of grass were grown on non-contaminated Palapye soil and mine tailings to obtain non-phytoremediation and phytoremediation biomasses, respectively. These biomasses were pyrolyzed at 550 °C in a nitrogen-flowing environment for 30 min. The chemical properties of the raw biomasses and subsequent biochars (pH, EC, biochar yield, syngas percentage, oil percentage, percentage fixed carbon, ash content, volatile matter, heavy metal contents, and functional groups) were analyzed and compared.

Results Biochars from phytoremediation biomasses displayed higher Al, Cu, Ni, Fe, Cr, Zn, biochar yield, ash content and volatile matter content but had low fixed carbon, pH, and electrical conductivity compared to biochar from non-phytoremediation biomasses. FTIR data of biochars subjected to principal component analysis extracted 2 principal components (PC) which contributed about 57.14% and 41.77% of data variance, corresponding to PC1 and PC2, respectively. PC1 was associated with primary alcohol, allene, thiocyanate, carboxylic acid, cyclic alkene, alkyne, and alkane. PC2 was associated with while alcohol contributed to PC2. PC1 had a very strong negative correlation with biochar pH and EC and ash content but had a strong positive correlation with Al. The biplot discriminated biochar samples based on both the grass types and the source of biomass. The biplot indicated an increase in identified functional groups from non-phytoremediation biochars to phytoremediation biochars except for *Cymbopogon citratus*. Biochars from the *Chrysopogon zizanioides* phytoremediation biochars showed low intensities of anatase and dolomite peaks. Biochars from phytoremediation biomasses had few pore cavities as compared to the non-phytoremediation biochars.

Conclusion Heavy metal contents of the phytoremediation biomasses from different plant species had altered the yield, chemical properties, and structural components of biochars.

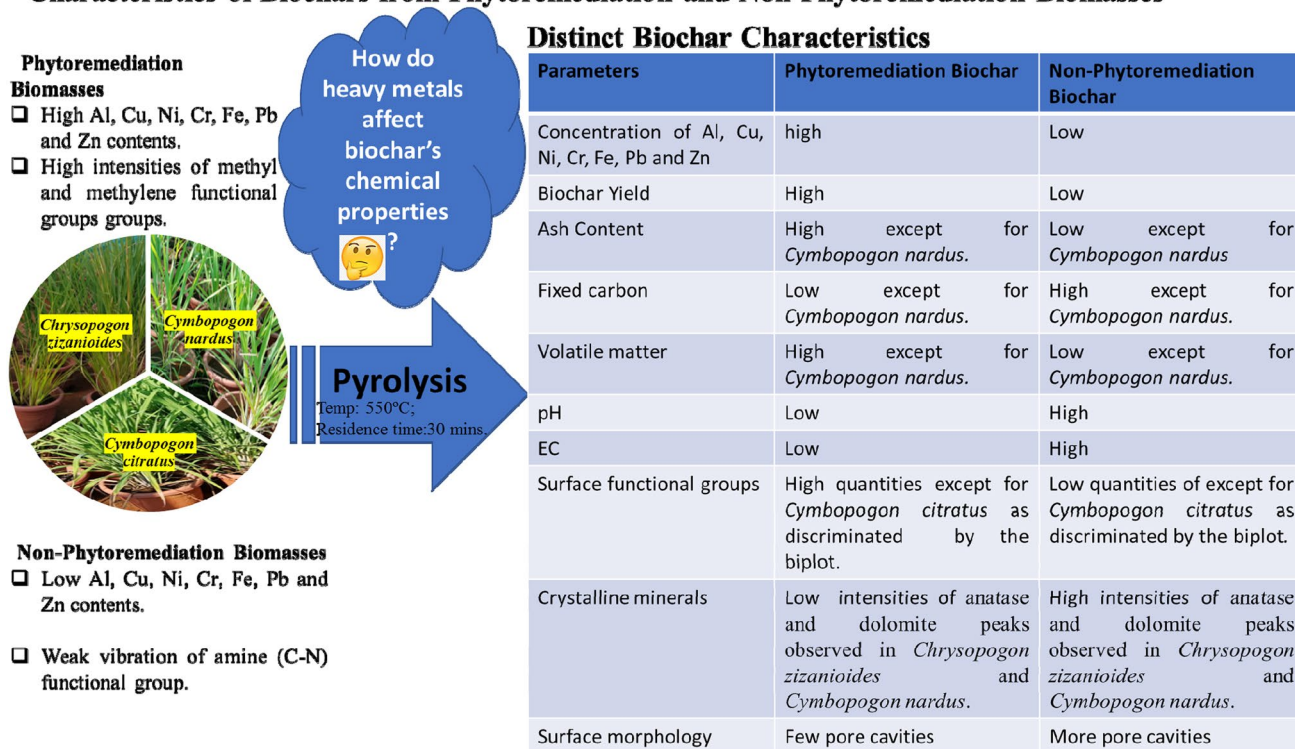
✉ Venecio U. Ultra Jr
Ultrav@biust.ac.bw

¹ Department of Earth, and Environmental Sciences, Botswana International University of Science and Technology, Palapye, Botswana

² Department of Chemical and Forensic Sciences, Botswana International University of Science and Technology, Palapye, Botswana

Graphical Abstract

Characteristics of Biochars from Phytoremediation and Non-Phytoremediation Biomasses



Keywords Biochar · Non-phytoremediation · Phytoremediation · Pyrolysis · Surface functional group

Statement of Novelty

This paper compared the chemical and structural characteristics of biochars derived from *Cymbopogon citratus*, *Cymbopogon nardus*, and *Chrysopogon zizanioides* phytoremediation biomasses with the non-phytoremediation counterpart. This is the first study that directly elucidated the differences in pH, EC, biochar yield, syngas percentage, oil percentage, percentage fixed carbon, ash content, volatile matter, heavy metal contents, functional groups, crystalline minerals, and surface morphology of biochars produced from phytoremediation and non-phytoremediation biomasses, simultaneously. To our knowledge, this is the first study to apply principal component analysis in discriminating the surface functional group characteristics of different biochar from different sources.

Introduction

Phytoremediation involves the utilization of plants for the sorption of contaminants from polluted soil or water. Recently, phytoremediation as a cost-effective and green

technology has caught the attention of many scientists due to its potential to remediate contaminated soil and water bodies, notably with respect to acid mine drainage [1]. Generally, plants grown in contaminated soils constitutes higher concentrations of HM in their tissues as compared to those plants grown in non-contaminated environment [2]. The highest heavy metal concentrations in phytoremediation biomass are attributed to the higher uptake of these elements from soil when its concentration and availability is high [3]. Some plants could have the ability to hyperaccumulate while others have the ability to exclude these metals and reduce uptake while others can render the metals in the vacuole [4]. As a consequence of the growing these plants in heavy metal contaminated soil, the contents of structural components of the plants such as the cellwall are altered by the accumulation of substances such as HM [5]. Changes to these components could decrease the plant's overall biomass and affect its morphological properties. The presence of HM in phytoremediation biomass could stimulate the phenolic secondary metabolic production pathway resulting in an increase to the lignin content, thereby enhancing the thickness of the cell wall [6]. Despite the potential of phytoremediation biomass to

remediate contaminated environments, there are issues associated with its usage such as heavy metal content and a high probability to transfer pollutants [7]. Accumulation of HM in phytoremediation plants is also a big concern as these plants provide a pathway for the transmission of toxic substances to animals and humans i.e., HM are introduced into the food chain when herbivores feed on these biomasses. Phytoextraction of HM is still of threat to the environment since microorganisms cannot degrade toxic metals. As such, heavy metal contaminated biomass needs proper handling [8]. Current methods of phytoremediation biomass disposal include direct disposal, composting, compaction, leaching, incineration, and pyrolysis.

Biochar is a solid carbon-rich product of pyrolysis that can be generated from different feedstocks such as agricultural and forest remains, industrial waste, grass, and less common materials like papers, bones, and even old tires [9]. Pyrolysis refers to the thermochemical technique that involves the conversion of the biomass into biochar, bio-oil and syngases at moderate temperature in an inert environment [10]. Unlike other methods, the pyrolysis method is capable of simultaneously recovering HM and achieving a greater degree of biomass reduction [11]. Biomass impregnated HM enhance the biomass pyrolysis by decreasing the pyrolysis activation energy [3]. Biochar yield and chemical attributes mainly rely on the type of biomass and the pyrolysis process [12]. Pyrolysis temperature is a crucial factor in biochar production since the release of condensable compounds and volatiles are temperature dependent [13]. The secondary char produced from chemical reaction between volatiles and primary char is a result of longer pyrolysis residence time [10]. Different grass species have different components of their structural components which affect the distributions of pyrolytic products (char, gases, bio-oil, and tar) [14]. Biomass heavy metal content may influence the chemical properties of obtained biochar [15]. After the pyrolysis of phytoremediation biomass at a low temperature, HM become enriched in biochar while syngas and liquid (bio-oil and tar) are altered to have the smallest proportions of HM [16].

This study aims to provide the missing information for the chemical and structural characteristics of the biochar which are produced from non-phytoremediation and phytoremediation biomasses of *Chrysopogon zizanioides*, *Cymbopogon citratus*, and *Cymbopogon nardus*. The specific objectives are: (i) to characterize the chemical composition of the raw materials; (ii) to determine the yield of biochar; and (iii) to determine some of the chemical properties such as pH, EC, volatile matter, fixed carbon, ash content, the surface functional groups, crystalline minerals, and surface morphology of biochar from non-phytoremediation and phytoremediation biomass of *Chrysopogon zizanioides*, *Cymbopogon citratus*, and *Cymbopogon nardus*. It is hypothesized that other

factors such as heavy metal content will have a distinct effect on the yield and chemical properties of biochar.

Materials and Methods

Sources of Biomasses

Three phytoremediation biomasses of *Cymbopogon citratus*, *Cymbopogon nardus*, and *Chrysopogon zizanioides* were obtained by growing these grasses in the mine tailings of Bamagwato Concessions Limited (BCL). Non-phytoremediation biomasses were produced from non-contaminated soil collected around the vicinity of the BIUST experiment station. The BCL mine tailings are highly acidic with high amounts of HM such as Cu, Ni, Pb, Mn, Zn and As with the following concentrations of 5311.62, 2025.22, 552.81, 1137.53, 220.27, and 154.31 mg/kg, respectively [17]. The pH of BCL Cu-Ni mine tailings is strongly acidic (pH: 2) with an electrical conductivity of 2.59 dS/m [18]. For phytoremediation biomass, plants were grown under greenhouse conditions for four months while the non-phytoremediation biomasses were grown outside the greenhouse. The pH and electrical conductivity of soil where non-phytoremediation biomasses were grown was 7.60 and 0.083 dS/m, respectively [19]. The concentrations of Fe, Cu, Mn, Ni, Zn, As, Cr and Pb in the soil were 15, 109.65, 76.22, 242.68, 153.50, 22.04, 2.32, 216.20 and 39.25 mg/kg, respectively [19].

The biomasses were harvested and taken to a laboratory for further treatment before pyrolysis. Samples were air-dried at room temperature (25 °C) for 72 h and oven-dried overnight at 105 °C. They were then ground using a Philips mixer grinder to obtain finer particles and subjected to pyrolysis.

Pyrolysis Conditions

For each batch, approximately 300 g of raw biomass was thermally heated in a 1-L batch reactor at 550 °C in a nitrogen-flowing environment for 30 min with a heating rate of 18 °C/minute. The condensable part of the product was condensed into a series of condensers: the first condenser (TK-02) was set at a temperature of 130 °C, the second condenser (TK-03) was set at a temperature of 80 °C and the third condenser (TK-04) was set to room temperature (25 °C), with each condenser collecting heavy oil, moderate oil, and pyrolysis liquids, respectively. For each raw material, three biochar preparations were performed. The resultant biochar was packaged and sealed in polyvinylchloride (PVC) bags to be used in the next phase of the study. Percentage biochar yield was calculated using the following formula:

$$BC(\%) = \frac{BC}{R_{wi}} * 100 \quad (1)$$

where: BC (%) is the biochar percentage yield, R_{wi} is the weight of raw biomass, And BC is the weight of biochar after pyrolysis.

Chemical Characterization of Raw Biomasses and Biochars

The heavy metal concentrations (Fe, Cu, Ni, Al, As, Cr, Pb, Cd, and Zn) of raw and biochar samples were measured after acid digestion of 0.5 g of biochar/raw biomass in a microwave digester (MA174—Milestone Ethos Easy) at 200 °C for 2 h using 2 ml of 30% H₂O₂ and 6 ml of concentrated HNO₃ followed by quantification using inductively coupled plasma-optical emission spectrometry (Thermo Scientific ICAP 7000 Series ICP–OES). The biochar pH and EC were measured in water suspension (1:20, biochar/water) after oscillation for 2 h using a portable pH/EC meter.

The fixed carbon (FC), volatile matter (VM), and ash contents of the biochar were determined by heating oven-dried biochar at 550 °C in a muffle furnace for 5 h, and the ash content, volatile matter, and fixed carbon were calculated as follows:

$$\text{Ash Content (\%)} = \left(\frac{W_2 - W_0}{W_1 - W_0} \right) \times 100 \quad (2)$$

$$\text{VM (\%)} = \left(\frac{W_1 - W_2}{W_1} \right) \times 100 \quad (3)$$

$$\text{FC(\%)} = 100 - (\text{VM(\%)} + \text{Ash content(\%)}) \quad (4)$$

where: W₀ is the weight of empty crucible (g), W₁ is the weight of crucible (g) plus the weight of biochar sample (g), W₂ is the weight of crucible (g) plus the weight of sample after furnace heating (g).

Surface Functional Groups Analysis

Surface functional groups of raw biomasses and biochars were recorded in the wavelength range of 650–4000 cm⁻¹ with a resolution of 4 cm⁻¹ using Fourier Transformer Infrared (FTIR) spectroscopy (USA Nicolet IS5). The infrared spectrum table was used to interpret the FTIR spectra.

X-Ray Diffraction Patterns of Raw Biomasses and Subsequent Ordinary Biochars

The crystalline minerals composition of the pulverized samples of the raw biomasses and ordinary biochar samples were analyzed using X-ray diffraction data derived from a

Bruker D8 Advance powder diffractometer, with a Cu X-ray source, and a LynxEye XE energy-dispersive strip detector. The instrument used a Cu-K α at a wavelength of 1.54056 Å and 2 θ between 10 and 80 degrees with steps of 0.02 degrees at a rate of 0.500 s/step. The machine was operated at 40 mA and 40 kv.

Scanning Electron Microscope Analysis of Ordinary Biochars

Ordinary and activated biochar samples were first coated with carbon and the density and shapes of the surface pores were characterized using a scanning electron microscope at a working distance, voltage, and magnification of 10 mm, 15.0 kV, and $\times 1700 \mu\text{m}$, respectively.

Statistical Analysis of the Data

The data was subjected to analysis of variance (ANOVA) for significant differences between 2 factors (grass types and biomass sources). When a significant difference identified, the mean comparison was performed using Turkey's homogeneity test at a 0.05 probability level. Surface functional group data was subjected to principal component analysis (PCA), and the functional groups which had PCA loadings above ± 0.8 was considered to be the functional groups contributing to the variability of the samples. Pearson correlations were conducted between chemical characteristics of raw biomasses and biochars, and with the PC loadings.

Results and Discussion

Heavy Metal Contents of Raw Biomasses

Heavy metals contents in non-phytoremediation and phytoremediation raw biomass significantly differed from each other and between grass types (Table 1). Regardless of the grass types, the phytoremediation biomasses had higher heavy metal content (Al, Pb, Cu, Zn, Fe, and Ni) than the non-phytoremediation biomasses. These results is parallel to the previous findings that heavy metal concentrations of biomass grown in a heavy metal contaminated environment was significantly higher than that of uncontaminated biomass [20]. In addition, grass species also contributed the difference of biomass characteristics between phytoremediation and non-phytoremediation. The Al concentration of non-phytoremediation biomasses is about 34.7–81.7 mg/kg while phytoremediation biomasses had an Al concentration range of 166.23–177.08 mg/kg with no significant difference between grass species in the phytoremediation group. Among non-phytoremediation biomasses, *Cymbopogon nardus* had the highest Al content (81.7 mg/kg) compared to

Table 1 Average heavy metal concentrations of non-phytoremediation and phytoremediation biomasses

Grass type	Source of biomass ^a	Al mg kg ⁻¹	Cr	Cu	Fe	Ni	Pb	Zn
<i>Chrysopogon zizanioides</i>	RV1	36.99c	0.79b	0.75d	18.45c	0.17b	0.30c	0.56c
	RV2	166.23a	1.12a	2.41b	142.52a	260.66a	0.61b	1.5a
<i>Cymbopogon nardus</i>	RC1	81.7b	0.00d	1.23 cd	36.85b	2.28b	0.16d	0.84bc
	RC2	177.08a	0.00d	4.50a	20.00c	27.92b	0.26 cd	1.25ab
<i>Cymbopogon citratus</i>	RL1	34.7c	0.00d	1.13 cd	12.59c	2.83b	0.70b	0.51c
	RL2	175.02a	0.53c	1.45c	17.31c	4.67b	1.08a	1.28a
P- values	TG	0.000***	0.000***	0.000***	0.000***	0.000***	0.000***	0.000***
	SB	0.000***	0.000***	0.000***	0.000***	0.000***	0.000***	0.000***
	TG * SB	0.002***	0.000***	0.000***	0.000***	0.000***	0.000***	0.000***

Means within the same column, followed by the same letter(s) are not significantly different according to Turkey's homogeneity test at 5% significance

^aRV1: *Chrysopogon zizanioides* non-phytoremediation biomass, RV2: *Chrysopogon zizanioides* phytoremediation biomass, RC1: *Cymbopogon nardus* non-phytoremediation biomass, RC2: *Cymbopogon nardus* phytoremediation biomass, RL1: *Cymbopogon citratus* non-phytoremediation biomass, and RL2: *Cymbopogon citratus* phytoremediation biomass

other grass species. *Chrysopogon zizanioides* exhibited the highest Cr concentration in both phytoremediation and non-phytoremediation biomasses. Chromium was not detected in the *Cymbopogon citratus* and *Cymbopogon nardus* non-phytoremediation biomasses. The Cu concentration of non-phytoremediation biomasses is about 0.75–1.23 mg/kg with the highest Cu concentration observed in *Chrysopogon zizanioides*. The phytoremediation biomasses displayed the Cu concentration range of 1.45–4.50 mg/kg with a higher significant value observed in *Cymbopogon nardus* (4.50 mg/kg) followed by *Chrysopogon zizanioides* (2.41 mg/kg) and *Cymbopogon citratus* (1.13 mg/kg). Among non-phytoremediation biomasses, Fe concentration was significantly higher in *Cymbopogon nardus* (36.85 mg/kg) while *Cymbopogon citratus* and *Chrysopogon zizanioides* displayed almost similar Fe concentrations. Amongst phytoremediation biomasses, *Chrysopogon zizanioides* had a significantly higher Fe concentration compared to *Chrysopogon zizanioides* and *Cymbopogon citratus* which had comparable Fe concentrations. Similarly, Mirecki et al. [21] observed that different plant types grown in the same soil comprised varying heavy metal concentrations.

There was a significant interaction effect between the type of grass and source of biomass on Ni concentrations with *Chrysopogon zizanioides* displaying significantly higher Ni concentration (260.66 mg/kg) compared to other grass species. The Pb concentration of non-phytoremediation biomasses ranged from 0.16 mg/kg to 0.70 mg/kg while phytoremediation biomasses had a Pb concentration range of 0.26–1.08 mg/kg with significant differences between grass types. *Cymbopogon citratus* indicated a higher Pb concentration in both non-phytoremediation and phytoremediation biomasses. The Zn concentration was slightly higher in *Cymbopogon nardus* for non-phytoremediation biomasses

(0.84 mg/kg) while no significant difference was observed between *Cymbopogon citratus* and *Chrysopogon zizanioides* (Table 1). Regarding phytoremediation biomasses, *Cymbopogon nardus* had lower Zn concentration while no significant difference in Zn concentration was observed between *Chrysopogon zizanioides* and *Chrysopogon citratus* (Table 1).

Variation in heavy metal concentrations between non-phytoremediation biomasses was attributed to the difference in HM uptake capacities of the grass species as a result of genetic variation [10]. Factors influencing the uptake capacity of metal by the plant include the difference in grass species, solubility of HM in soil the solution, and HM translocation from the soil solution into the plant [22]. Plants adjust their roots in the rhizosphere by excreting exudates which modify the solubility of HM, making it easier for their adsorption. Such physiologic responses differed from one species to another, and from the physiochemical characteristics of the soil and the microenvironment. These differences in the composition of exudates between plant species will contribute to the difference in uptake of HM amongst plant species [23]. The study conducted by Kriti et al. [24], indicated that *Chrysopogon zizanioides* had the bioaccumulation factor (BAF) of 0.80 for Ni and 0.24 for Cd while *Cymbopogon citratus* had a BAF of 0.35 for Ni and 0.14 for Cd when grown in 4% Ni–Cd battery electrolyte waste-contaminated soil. The reason for higher heavy metal content in phytoremediation biomasses is that BCL Cu–Ni mine tailings contained higher heavy metal content which was available for bioaccumulation by grass species as compared to Palapye-BIUST soil where non-phytoremediation biomasses were obtained. Variation in the HM adsorbed by three phytoremediation plant species could be ascribed to the difference in HM transport channels of

these plant species. Some of the heavy metal transporters include the cation diffusion facilitator (CDF) family, heavy metal-transporting ATPases, natural resistance-associated macrophage protein (Nramp), metal transport proteins, and the Zinc-Tron permease (ZIP) family. Nramp transporters are responsible for the translocation of bivalent metals (Cd^{2+} , Fe^{2+} , Co^{2+} , Mn^{2+} , Cu^{2+}) from the plant roots to the shoots. Metal transport proteins carry Ni and Zn while heavy metal-transporting ATPases are responsible for the transportation of Pb, Co, Cd, and Zn in plants [25]. These results confirmed the existence of variability in the heavy metal contents of the biomasses grown from contaminated and non-contaminated substrates and these variations are also dependent on the grass species. It is expected that variation in the chemical composition of the raw materials will be carried over into their respective biochar products.

Heavy Metal Contents of Biochar

Biochars displayed higher Al, Cr, Cu, Fe, Ni, Pb, and Zn concentrations compared to their respective raw biomasses (Table 2). However, Cr was not detected in the biochar from the *Cymbopogon nardus* non-phytoremediation and phytoremediation biomasses, and in the biochar from the *Chrysopogon zizanioides* non-phytoremediation biomass. A similar trend with that of the raw biomasses was observed for biochar samples with higher heavy metal contents of biochars from phytoremediation biomasses, compared to biochars derived from non-phytoremediation biomasses, regardless of the grass species. Specifically, biochar from

the *Cymbopogon nardus* phytoremediation biomass displayed significantly higher Al concentration (470.69 mg/kg) which was 62% higher than the corresponding raw biomass, when compared to other grass species. Biochar from the *Chrysopogon zizanioides* phytoremediation biomass had significantly higher Cr (1.60 mg kg⁻¹), Cu (23.27 mg kg⁻¹) Fe (170.92 mg kg⁻¹), Ni (285.66 mg kg⁻¹) and Zn (4.30 mg kg⁻¹) concentrations compared to other grass species which were 30%, 89.6%, 16.6%, 8.6%, and 65.1% higher than the corresponding raw biomasses, respectively. There was no significant difference between the source of the biomass and grass types for Zn concentrations. Biochar from the *Cymbopogon citratus* phytoremediation biomass displayed a significantly higher Pb (1.52 mg/kg) concentration compared to *Cymbopogon nardus* and *Chrysopogon zizanioides* which was 29% higher than the corresponding raw biomass. These results corroborated the findings of Wang et al. [26], who reported that at the temperature range of 300 to 700 °C, HM in biochars were retained to approximately within the range of 91.1–97.49% for Cu, Cr, Ni, Zn, and Mn. The high retention of these metals in the biochars was attributed to differences in the volatilization rate between these metals and the organic components of the raw materials. Organic substances are volatilized more readily than HM. Thus, the HM are retained in the biochar [6]. The high pyrolysis temperature causes excitement of electrons which results in the loss of chemical bonds between HM and organic compounds, thus releasing the organic compounds through volatilization and consequently enriching the concentrations of HM in the biochar matrix. The Cr, Cu, Ni, Pb,

Table 2 Average heavy concentrations of biochar from non-phytoremediation and phytoremediation biomasses

Grass type	Source of biomass ^a	Al mg kg ⁻¹	Cr	Cu	Fe	Ni	Pb	Zn
<i>Chrysopogon zizanioides</i>	BCV1	87.07d	1.01b	2.27c	22.44d	3.83c	0.41 cd	2.52b
	BCV2	183.78c	1.60a	23.27a	170.92a	285.24a	0.94c	4.30a
<i>Cymbopogon nardus</i>	BCC1	323.10b	0.00d	6.91b	38.75c	4.01c	0.70bc	2.89b
	BCC2	470.69a	0.00d	8.99b	72.11b	25.61b	0.24d	4.15a
<i>Cymbopogon citratus</i>	BCL1	44.65e	0.00d	2.60c	31.82 cd	5.55c	0.71bc	2.34b
	BCL2	188.78c	0.007c	3.20c	27.49d	8.82c	1.52a	3.74a
SB average	Non-phytorem	151.61	0.34	3.93	31.00	4.46	0.61	2.58
	phytorem	281.08	0.54	11.82	90.17	106.56	0.90	4.06
IBI permissible limits (mg kg ⁻¹)		ND	93–1200	143–6000	ND	47–420	121–300	416–7400
P- values	TG	0.000***	0.000***	0.000***	0.000***	0.000***	0.000***	0.18 ns
	SB	0.000***	0.000***	0.000***	0.000***	0.000***	0.000***	0.000***
	TG * SB	0.002***	0.000***	0.000***	0.000***	0.000***	0.000***	0.58 ns

Means within the same column, followed by the same letter(s) are not significantly different according to Turkey's homogeneity test at 5% significance

^aBCV1: *Chrysopogon zizanioides* non-phytoremediation biochar, BCV2: *Chrysopogon zizanioides* phytoremediation biochar, BCC1: *Cymbopogon nardus* non-phytoremediation biochar, BCC2: *Cymbopogon nardus* phytoremediation biochar, BCL1: *Cymbopogon citratus* non-phytoremediation biochar and BCL2: *Cymbopogon citratus* phytoremediation biochar, SB: source of biomass, TG: type of grass, IBI: International Biochar Initiative, ND: not defined

and Zn concentrations of the current study were within the International Biochar Initiative permissible limits that are defined in the literature review [27]. The permissible limits for Al and Fe levels in biochar have not been defined.

Biochar Yield and Yield Components

The biochar percentage yield of non-phytoremediation biomass ranged from 30.56 to 32.29% with the highest biochar yield value observed in *Cymbopogon citratus* followed by *Chrysopogon zizanioides* (31.94%) and *C. nardus*, respectively (Table 3). The difference in biochar yields from non-phytoremediation biomasses could be attributed to the difference in cellular components of each species [22]. The percentage yield of biochars from phytoremediation biomasses ranged from 31.11 to 37.53% which was higher than those biochars from non-phytoremediation biomasses except for *Chrysopogon zizanioides*. Similarly, He et al. [2] and He et al. [28], reported that the presence of HM in the feedstock increased biochar yield. Amongst phytoremediation biochars, the yield was highest in *Cymbopogon citratus* followed by *Chrysopogon zizanioides* (31.76%) and *Cymbopogon nardus*. The higher percentage biochar yield of biochars from phytoremediation biomass is due to the presence of HM as they form part of non-volatile, incombustible (inorganic) constituents thus increasing the mass of the biochar. The highest percentage biochar yield of biochar from *Cymbopogon citratus* phytoremediation biomass could be ascribed to high lignin content. According to Tomczyk et al. [23], high lignin content favors higher biochar production as opposed to cellulose and hemicellulose contents. The

higher molecular weight and hydrophobicity of the lignin component make its structure resistant to breakdown and volatilization [25].

The liquid yield was not significantly affected by the interaction between grass type and sources. Rather, only the main effect due to the source of the biomass was observed. On average, the liquid yield from the pyrolysis of the phytoremediation biomasses was significantly lower than the non-phytoremediation biomasses indicating that HM in the raw biomass will decrease the liquid yield even at 550 °C pyrolysis temperature. The results of the current study do not agree the results reported by Han et al. [3] which revealed that biomass impregnated HM increased the liquid yield. Stimulation of phenolic secondary metabolic synthesis pathway due to HM stress of the raw biomass increases its lignin content in the secondary cell thereby increasing cell wall thickness [6]. According to Jung et al. [29], cellulose and hemicellulose pyrolysis produce more bio-oil compared to lignin hence the low pyrolysis liquid yield of this current study could be contributed to dominant lignin composition of the raw biomass stimulated by the presence of HM.

There were no significant interaction effects on the syngas yield observed between the type of grass and source of the biomass, except for the source of the biomass alone. The syngas yield from the pyrolysis of phytoremediation biomasses was lower compared to the non-phytoremediation biomasses except for *Cymbopogon citratus*. The difference in the syngas yield between non-phytoremediation and phytoremediation biomass could be attributed to the high amount of biochar produced with a respect to the overall product components. At the working temperature of this

Table 3 Pyrolysis products and biochar chemical composition derived from phytoremediation and non-phytoremediation grasses

		Pyrolysis products				Biochar properties			
		BC (%)	Liquid (%)	Syngas (%)	Ash (%)	FC (%)	Vm (%)	pH	EC (µS/cm)
<i>Chrysopogon zizanioides</i>	BCL1	31.94b	32.41a	48.62a	17.57a	71.00a	11.43a	10.8a	4440a
	BCL2	31.76b	29.38a	44.23a	25.23a	60.97a	13.80a	10.2a	3200b
<i>Cymbopogon nardus</i>	BCC1	30.56b	32.41a	43.84a	17.50a	68.62a	13.88a	9.5a	1120c
	BCC2	31.11b	29.38a	39.12a	12.45a	74.23a	13.32a	9.3a	960c
<i>Cymbopogon citratus</i>	BCV1	32.29b	30.00a	38.21a	17.83a	66.25a	15.52a	10.25a	1375c
	BCV2	37.53a	27.41a	41.56a	21.09a	62.65a	16.26a	9.70a	1080c
SB Averages	Non-phytorem	31.63b	31.67a	43.55a	17.63b	68.51a	13.86b	10.18a	2311a
	Phytorem	33.47a	28.72b	41.64b	19.59a	66.20b	14.21a	9.73b	1746b
P Values	TG	0.020***	0.11 ns	0.45 ns	0.18 ns	0.070 ns	0.55 ns	0.28 ns	0.000***
	SB	0.000***	0.000***	0.000***	0.000***	0.000***	0.000***	0.000***	0.000***
	TG*SB	0.020***	0.46 ns	0.37 ns	0.14 ns	0.056 ns	0.43 ns	0.28 ns	0.000***

^aBCV1: *Chrysopogon zizanioides* non-phytoremediation biochar, BCV2: *Chrysopogon zizanioides* phytoremediation biochar, BCC1: *Cymbopogon nardus* non-phytoremediation biochar, BCC2: *Cymbopogon nardus* phytoremediation biochar, BCL1: *Cymbopogon citratus* non-phytoremediation biochar and BCL2: *Cymbopogon citratus* phytoremediation biochar: BC (%): biochar percentage yield, EC: electrical conductivity, VM: volatile matter, FC: fixed carbon, SB: source of biomass and TG: type of grass

study, biochar is more favored than syngas formation which usually occurs at a temperature above 1000 °C [16]. Ideally, the effect of higher raw biomass heavy metal content on syngas production could be observed at high temperatures wherein the presence of HM increases syngas production due to the catalytic effect during pyrolysis.

Biochar Components

The ash content of biochar was not significantly affected by the interaction between grass type and sources. Rather, only the predominant effect due to the source of the biomass was observed. On average, the ash content of biochar from non-phytoremediation biomasses was about 17.63% ranging from 17.50 to 17.83% while those from phytoremediation biomass was about 19.59% with a percentage range of 12.45–25.23%. The increase in ash content of biochar from phytoremediation biomasses could be attributed to higher heavy metal loads which contribute to an increase in incombustible compounds of the biomass after pyrolysis. Inorganic compounds such as Mg, K, Ca, and P contribute to the ash content of plant biomasses [30].

The fixed carbon content of biochar was not significantly affected by the interaction between grass type and sources, only the main effect due to the source of the biomass was observed. On average, the percentage of fixed carbon of biochars from phytoremediation biomasses was lower than that of biochars from non-phytoremediation biomasses. The high percentage of fixed carbon in biochar indicates that the matrix still contains some original organic plant residue [23]. During pyrolysis, the lignin component volatilizes at low rates as compared to hemicellulose and cellulose contents which may result in high fixed carbon content. Ideally, the HM induce lignin formation in plants and consequently increase the fixed carbon of biochar from the phytoremediation biomass [31]. This study found the opposite which could imply that in this pyrolysis condition, high heavy metal content will result in a decrease in the fixed carbon formation during pyrolysis. The low fixed carbon content of biochar from phytoremediation biomass suggests that the presence of HM in the raw biomass favors the high transformation rate of plant original organic compounds into the volatile matter.

There was no significant interaction between the type of grass and the source of biomass of volatile matter content. Only the source of the biomass had a significant influence on the percentage of volatile matter content. On average, the volatile content of biochars from phytoremediation biomasses was higher compared to biochars from non-phytoremediation biomasses except for *Cymbopogon nardus*. The cellulose, hemicellulose, and lignin contents of the raw biomass influence the rate of volatile matter loss in the plant. During pyrolysis, cellulose and hemicellulose devolatilize

rapidly while lignin devolatilizes at a slow rate [32]. The higher volatile matter of biochar from phytoremediation biomass is due to the catalytic effect of the HM which promoted the decomposition of cellular components of the biomass [2]. Metals such as Cu, Fe, and Zn catalyze the decomposition of lignocellulose hence speeding up the devolatilization rate of cellular components of the grass biomasses [28, 32].

pH and EC of Biochar

The interaction effect between the type of grass and the source of the biomass on biochar pH was insignificant. The biochars derived from phytoremediation biomasses had alkaline pH with an average pH value of 9.73 while the pH of biochar solutions of biochars from non-phytoremediation biomasses was more alkaline with an average pH value of 10.25. Du et al. [33] observed an alkaline biochar pH (10.38) of biochar derived from *Symphytum officinale* L. phytoremediation biomass. According to the report by Zeng et al. [34], biochars from four phytoremediation biomasses (*S. rosthorni* seemen, *T. dealbata*, *V. zizanioides* and *Phragmites* sp.) produced at 500 °C had an alkaline pH value (pH range: 10.20–10.77) and these results are consistent with the findings of the current work. This suggests that hydrogen ions from hydrolysis of heavy metal in the biochar from phytoremediation biomasses could have contributed to the slight decrease in biochar pH. The alkaline pH of biochars from non-phytoremediation biomasses could be attributed to the released basic cations such as Mg^{2+} and Ca^{2+} during the thermal decomposition of the raw biomasses [35]. Mineral nutrients such as Mg, Na, K, and Ca in ash exist in the form of carbonates or oxides which are alkaline after dissolution in water [36]. Oxygen-containing acidic functional groups add to the acidity of biochar. During pyrolysis, the oxygen from O-containing acidic functional groups is lost, acidifying the pH of the biochar slurry.

Significant interaction effect existed between the type of grass and the source of biomass on the electrical conductivity of biochar samples. Biochar from *Chrysopogon zizanioides* displayed higher electrical conductivity for both non-phytoremediation (4440 $\mu S/cm$) and phytoremediation biomasses (3200 $\mu S/cm$) when compared to other grass species. The average EC of biochars from non-phytoremediation biomasses ranged from 1120 to 4440 $\mu S/cm$ while the EC of biochars from phytoremediation biomasses ranged from 960 to 3200 $\mu S/cm$ which was significantly lower than that of biochars from non-phytoremediation biomasses. The difference in the EC values between grass types could be due to the difference in soluble salts assimilated into their structures during plant growth [37]. High electrical conductivity is positively correlated with high nutrient absorption by plants [38]. The low EC values of biochars from phytoremediation biomasses could be ascribed to nutrient

deficiency due to competition between HM and plant nutrients for absorption and translocation [39]. Heavy metal speciation forms in biochar can be divided into four fractions: residual fractions, exchangeable fractions, reducible fractions, and oxidizable fractions. Reducible fractions include hydrous oxides, Mn, and Fe oxides. Metal oxides formed in the biochar matrix of phytoremediation biochars could have contributed to low biochar EC due to fewer ions in an aqueous solution to conduct electrical currents.

Relationship Between Pyrolysis Products, Biochar Components, and Heavy Metals of Raw Biomasses

Biochar yield had a moderate positive correlation with Al ($r=0.491$), ash ($r=0.513$), and volatile matter ($r=0.546$) content but displayed a strong positive correlation with Cu ($r=0.72$) as shown in Table 4. Liquid yield displayed a very weak inverse relationship ($r=-0.13$) but had a moderate inverse relationship with Al ($r=-0.40$), Fe ($r=-0.42$), and Ni ($r=-0.45$). A strong negative correlation ($r=-0.64$) was observed between liquid yield and Cu. Syngas yield displayed a very weak positive relationship with Al (0.13), Cr (0.15), and Zn (0.02) and a positive correlation with Cu (0.25), Fe (0.21) and Ni (0.22).

Ash content indicated an inverse relationship with Cr (-0.16) and a weak negative correlation with Zn (-0.22) Al ($r=0.13$), Cr $r=0.15$), Fe ($r=0.21$), Ni ($r=0.22$). Ash content had a weak positive correlation with Fe ($r=0.26$), Ni ($r=0.28$), Al ($r=0.29$), Pb ($r=0.31$) and Cu ($r=0.33$).

Volatile matter content had a weak positive relationship with Fe ($r=0.26$), Ni ($r=0.27$), Al ($r=0.28$), Pb ($r=0.33$) and Cu ($r=0.36$). Volatile matter content displayed a weak negative correlation with Cr (-0.14) and Zn (-0.19). Fixed carbon content showed a weak inverse correlation with correlated with Al (-0.28), Cu (-0.36), Fe (-0.26), Ni (-0.27), and Pb (-0.33) but indicated a weak positive correlation with Cr (0.14) and Zn (0.19).

Relationship Between Biochar Components, Chemical Properties, and Inherent Heavy Metals

Biochar yield displayed a very weak negative correlation with Zn ($r=0.11$) but displayed a moderate negative correlation ($r=-0.52$) with Al as depicted in Table 5. A moderate positive correlation ($r=0.48$) was observed between biochar yield and Pb. Biochar yield displayed a strong association with Cu ($r=0.720$) and Ni ($r=0.774$). Biochar pH had a very weak inverse relationship with Cr ($r=-0.12$) and a weak negative correlation with Ni ($r=-0.36$). Biochar pH had a moderate negative correlation with Fe ($r=-0.483$) and Cu ($r=-0.544$). A strong negative correlation was observed between biochar pH and Al ($r=-0.789$). Biochar pH displayed a weak positive correlation with Pb ($r=0.23$). Biochar electrical conductivity had a moderate inverse relationship with Cr ($r=-0.40$), Ni ($r=-0.42$), Fe ($r=-0.501$) and Cu ($r=-0.511$). A moderate negative correlation was observed between biochar EC and Al

Table 4 Pearson's correlation coefficients between pyrolysis products, biochar components and heavy metal concentrations of raw biomasses

Pyrolysis products	Heavy metal concentrations (mg kg ⁻¹)						
	Al	Cr	Cu	Fe	Ni	Pb	Zn
BC (%)	0.491*	0.00	0.720**	0.40	0.45	0.06	-0.02
Liquid (%)	-0.40	-0.13	-0.637**	-0.42	-0.45	0.13	-0.01
Syngas (%)	0.13	0.15	0.25	0.21	0.22	-0.18	0.02
Ash	0.29	-0.16	0.33	0.26	0.28	0.31	-0.22
VM	0.28	-0.14	0.36	0.26	0.27	0.33	-0.19
FC	0.28	0.14	-0.36	-0.26	-0.27	-0.33	0.19

BC biochar, VM volatile matter, and FC: fixed carbon

Table 5 Pearson's correlation coefficient between biochar components, chemical properties, and heavy metal contents

Biochar chemical parameters	Heavy metal concentrations (mg kg ⁻¹)						
	Al	Cr	Cu	Fe	Ni	Pb	Zn
BC (%)	-0.523*	0.652**	0.720**	0.626**	0.774**	0.480*	-0.11
pH	-0.789**	-0.12	-0.544*	-0.483	-0.36	0.23	-0.551*
EC (μS/cm)	-0.614**	-0.40	-0.511*	-0.501*	-0.42	0.26	-0.565*
Ash	-0.545*	0.32	0.33	0.45	0.502*	-0.14	-0.06
VM	-0.534*	-0.31	0.36	0.470*	0.519*	-0.09	-0.04
FC	0.534	0.31	-0.36	-0.470*	0.519*	0.09	0.04

BC biochar, EC electrical conductivity, VM volatile matter, FC fixed carbon

($r = -0.614$). A weak positive relationship between biochar pH and Pb ($r = 0.26$) was observed.

Ash content displayed a very weak inverse relationship with Zn ($r = 0.06$) and Pb (-0.14) but indicated a moderate negative correlation with Al ($r = -0.55$). Ash content had a weak positive relationship with Cr ($r = 0.32$) and Cu (0.33) but displayed a moderate positive association with Fe ($r = 0.45$) and Ni ($r = 0.50$). Volatile matter content displayed a very weak negative correlation with Pb ($r = -0.09$

and Zn ($r = -0.04$) and Cr had a weak inverse relationship ($r = -0.31$) with volatile matter content. A moderate negative correlation ($r = -0.50$) was observed between Al and volatile matter content. Cu had a weak positive association ($r = 0.36$) with volatile matter content while Cu displayed a moderate positive association with volatile matter content. Fixed carbon content had a weak negative correlation with Cu ($r = -0.34$) but displayed a moderate inverse relationship with Fe ($r = -0.47$). Fixed carbon content had a very weak positive correlation with Zn ($r = 0.04$) and Pb ($r = 0.09$) but displayed a moderate positive relationship with Al (0.53) and Ni ($r = 0.52$) (Table 6).

Table 6 Pearson correlation coefficients between the scores of different principal components extracted from PCA of functional groups of biochar and chemical properties of biochar

Factor	PC1	PC2
pH	-.872*	0.342
EC	-.827*	0.068
Ash	-0.791	-0.304
VM	-0.796	-0.362
FC	0.796	0.362
Al	0.668	-0.185
Cr	0.13	-0.069
Cu	0.34	-0.509
Fe	0.139	-0.72
Ni	0.075	-0.67
Pb	0.029	-0.152
Zn	0.465	-0.385

EC electrical conductivity, PC principal component, VM volatile matter, FC: fixed carbon

Functional Groups of Raw Biomasses and Biochar from FTIR Analysis

Surface group analysis data is shown in Figs. 1, 2, and 3. The peak at 1029 cm^{-1} was assigned to amine (C–N) stretching vibration such as epinephrine and dopamine which is in the same region with the aromatic C–H deformations and C–O, C–C stretching as well as C–OH bending modes in polysaccharides. The small transmittance band at 1164 cm^{-1} was attributed to the stretching vibration of the C–O bond in tertiary alcohol such as α -terpineol or C–H in plane deformation of the guaiacyl unit of lignin [40]. The transmittance band at 1230 cm^{-1} belonged to the amine (C–N) functional group, C–C, C=O, or C–O stretching modes in lignin with a high intensity of the band observed in *Cymbopogon nardus*

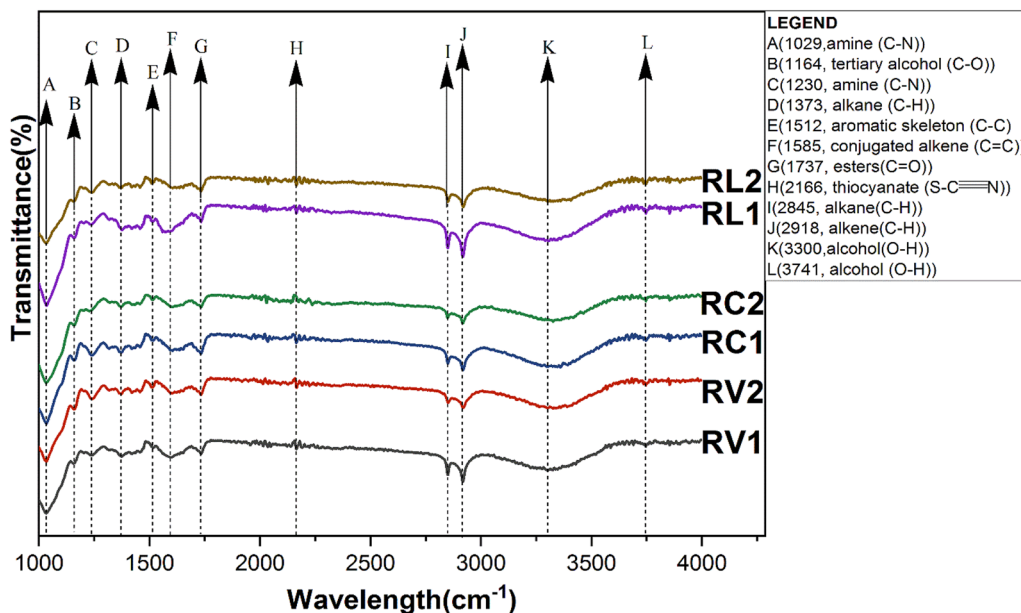


Fig. 1 Surface functional groups of non-phytoremediation and phytoremediation biomasses. RV1: *Chrysopogon zizanioides* non-phytoremediation biomass, RV2: *Chrysopogon zizanioides* phytoremediation biomass, RC1: *Cymbopogon nardus* non-phytoremediation

biomass, RC2: *Cymbopogon nardus* phytoremediation biomass, RL1: *Cymbopogon citratus* non-phytoremediation biomass, and RL2: *Cymbopogon citratus* phytoremediation biomass

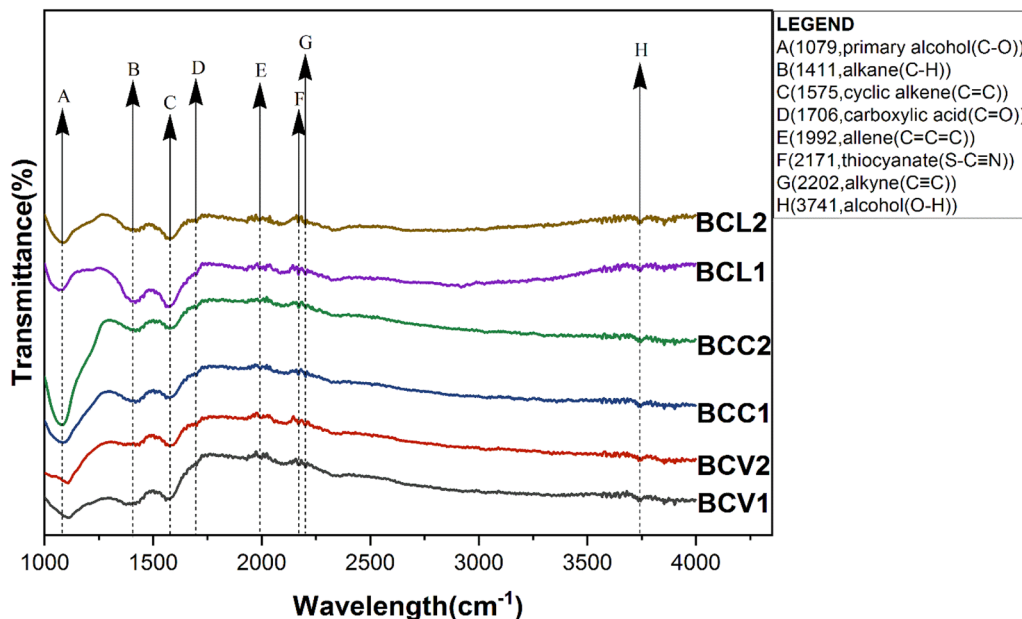


Fig.2 Surface functional groups of biochar from non-phytoremediation and phytoremediation biomasses. BCV1: *Chrysopogon zizanioides* non-phytoremediation biochar, BCV2: *Chrysopogon zizanioides* phytoremediation biochar, BCC1: *Cymbopogon nardus*

non-phytoremediation biochar, BCC2: *Cymbopogon nardus* phytoremediation biochar, BCL1: *Cymbopogon citratus* non-phytoremediation biochar and BCL2: *Cymbopogon citratus* phytoremediation biochar

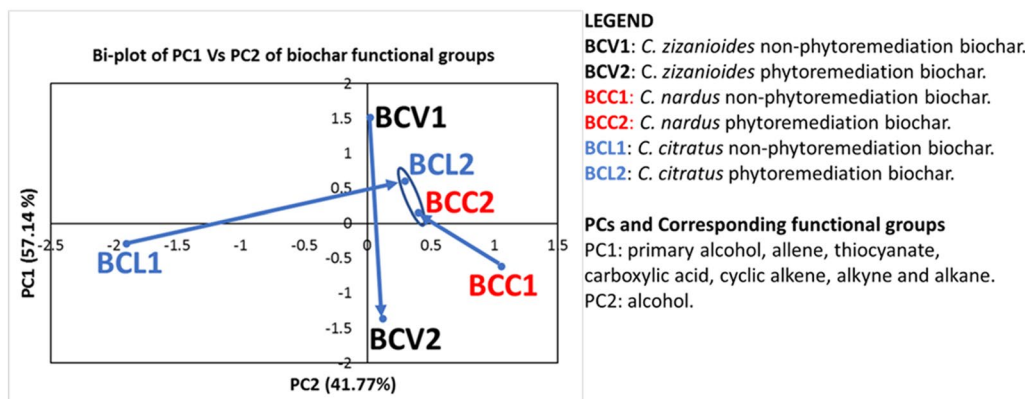


Fig.3 Biplot of PC1 vs PC2 extracted from the PCA of the functional groups of biochar derived from phytoremediation and non-phytoremediation grasses

amongst grass species. In comparison, the intensity of this peak slightly increased from non-phytoremediation biomass to phytoremediation biomass with the exception of *Cymbopogon nardus*. This suggests that HM present in phytoremediation biomasses induced the amine functional group of the raw biomasses except for *Cymbopogon nardus*. A small transmittance band at 1373 cm^{-1} may be assigned to C–H bending modes and the 1512 cm^{-1} bands were assigned to aromatic skeleton vibrations [41–43]. The peak at 1585 cm^{-1} was assigned to C=C stretching vibration caused by the aromatic structure and the band at 1737 cm^{-1} may be due to C=O stretching modes of carbonyl groups of carboxylic

acids and esters such as lactones. The stretching vibration of the thiocyanate (S–C≡N) functional group was observed at 2166 cm^{-1} .

Sharp bands observed at 2845 cm^{-1} and 2918 cm^{-1} were assigned to asymmetric and symmetric C–H stretching of methyl and methylene groups respectively or amine (N–H) stretching modes from primary amines. This bands at 2850 cm^{-1} and 2918 cm^{-1} are related to the C–H stretching vibrations of methyl and methylene groups [44]. The intensity of these functional groups amongst grass species descended as follows: *Cymbopogon citratus* > *Chrysopogon zizanioides* > *Cymbopogon nardus*. In comparison, the

peak intensities of these two functional groups decreased from non-phytoremediation biomass to phytoremediation biomass. This could be attributed to the reduction in peak transmittance due to HM load [45].

There was a change in the functional groups profile after the pyrolysis of non-phytoremediation and phytoremediation biomasses. These results corroborate the findings of the previous studies [33, 43] as they determined that pyrolysis of the raw biomass or feedstock results in alteration of the FTIR spectra. A pyrolysis temperature range of 350–650 °C results in the breaking of chemical bonds of the biomass and rearrangement of these bonds to form new functional groups [23]. Pyrolysis at high temperatures results in the degradation of hemicellulose, cellulose and lignin resulting in the reduction or complete disappearance of peaks associated with functional groups in these compounds [46]. The broad transmittance band at 1075 cm^{-1} was assigned to the stretching mode of the C–O bond of primary alcohols such as methanol and propanol. The intensity of this functional group was higher in biochar from *Cymbopogon nardus* phytoremediation biomass when compared to the corresponding biochar from non-phytoremediation biomass. Broad bands formed at 1411 and 1575 cm^{-1} were attributed to the aliphatic bending vibration of a methyl group (C–H) or O–H bending modes and stretching vibration of cyclic alkene (C=C), respectively. The intensity of the C=C functional group band was observed to be higher in biochar from *Cymbopogon citratus* non-phytoremediation biomass when compared to other grass species. A weak transmittance band formed at 1706 cm^{-1} was assigned to the stretching vibration of the C=O group of carboxylic acids such as 1-aminocyclopropane-1-carboxylic acid. Small peaks which formed at 1992 cm^{-1} , 2171 cm^{-1} and 2202 cm^{-1} belonged to the stretching vibrations of allene (C=C=C), thiocyanate (S–C≡C), and alkyne (C≡C) functional groups, respectively. A weak transmittance band at 3741 cm^{-1} belonged to the non-hydrogen bonded O–H functional group of alcohols. The band formation became enhanced across all samples after pyrolysis of the raw biomasses. The previous studies [20, 45] observed the broad band between a wavelength range of 3100–3600 cm^{-1} and attributed the band to hydrogen bonded O–H groups present in carbohydrates.

Surface functional group data of biochars subjected to PCA resulted in the extraction of 2 PCs which contributed about 57.14% and 41.77% of data variance, corresponding to PC1 and PC2, respectively. PC1 was associated with primary alcohol, allene, thiocyanate, carboxylic acid, cyclic alkene, alkyne, and alkane while PC2 was associated with secondary alcohol (Fig. 3). The biplot was able to discriminate biochar samples based on both types of grass species and the source of biomass. The biplot indicates an increase in the identified functional groups from non-phytoremediation biochars to phytoremediation biochars for *Cymbopogon nardus* and

Chrysopogon. zizanioides while opposite effects occurred in *Cymbopogon citratus*. Biochar from *Cymbopogon nardus* and *Cymbopogon citratus* phytoremediation biomasses had almost the same values of a primary alcohol, allene, thiocyanate, carboxylic acid, cyclic alkene, alkyne and alkane, and alcohol functional groups.

X-Ray Diffraction Patterns of Raw Biomasses and Subsequent Ordinary Biochars

Figure 4 displays the X-ray diffraction patterns of phytoremediation and non-phytoremediation biomasses. Amorphous carbon (002) was observed at 2θ range of 20–30° while talc (006) peaks formed at 2θ values of 28.8° and 40.8° in the *Chrysopogon zizanioides* non-phytoremediation and phytoremediation biomasses. As a function of height, *Chrysopogon zizanioides*, non-phytoremediation and phytoremediation biomasses had an intense talc peak as opposed to amorphous carbon peaks. According to [47], the broadness of the peaks at 2θ range of 20–30° is attributed to the presence of cellulose, hemicellulose, and lignin components. Sharp antigorite peaks at 2θ value of 32.1° were observed in biochar from *Cymbopogon nardus* and *Cymbopogon citratus*. The antigorite peak in *Cymbopogon citratus* non-phytoremediation and phytoremediation biochars was prominent, while *Cymbopogon nardus* non-phytoremediation biochar showed a weak peak. Calcite showed a small peak in the *Chrysopogon zizanioides* phytoremediation biomass. Sharp dolomite peaks were observed in *Cymbopogon nardus* and *Cymbopogon citratus* at 2θ value of 43.8°. It appears that the composition of the minerals available in the raw biomass differed between species and their growing condition (i.e., BCL tailings vs ordinary soil) which could be ascribed on their inherent genetic make-up and the concentration of these elements in soil. The genetic traits influencing the mineral composition of the grass species include their capacity to solubilize, absorb, translocate, bioaccumulate, and use mineral elements [48]. Similarly, the amount of the nutrients taken up by plants also depend on the quantity and intensity factors in soil [46, 49].

There was an increase in X-ray diffraction peaks after pyrolysis of the raw biomasses (Fig. 5). Previous studies indicated an evolution of new X-ray peaks due to the pyrolysis effect [2, 47]. An increase in mineral peaks after pyrolysis of the raw biomass indicates the enhancement of aromatic order indicating an increase in crystallization [48]. Non-phytoremediation and phytoremediation biochars from *Cymbopogon citratus* exhibited the sharp dolomite peaks, followed by non-phytoremediation biochar from *Cymbopogon nardus* while phytoremediation biochar from *Cymbopogon nardus* showed a weak peak of dolomite mineral. The difference in mineral phases of biochars from different grass types is a carry-over effect of the inherent

Fig.4 Crystalline minerals composition of non-phytoremediation and phytoremediation biomasses. RV1: *Chrysopogon zizanioides* non-phytoremediation biomass, RV2: *Chrysopogon zizanioides* phytoremediation biomass, RC1: *Cymbopogon nardus* non-phytoremediation biomass, RC2: *Cymbopogon nardus* phytoremediation biomass, RL1: *Cymbopogon citratus* non-phytoremediation biomass, and RL2: *Cymbopogon citratus* phytoremediation biomass. C: amorphous carbon, Ta: talc

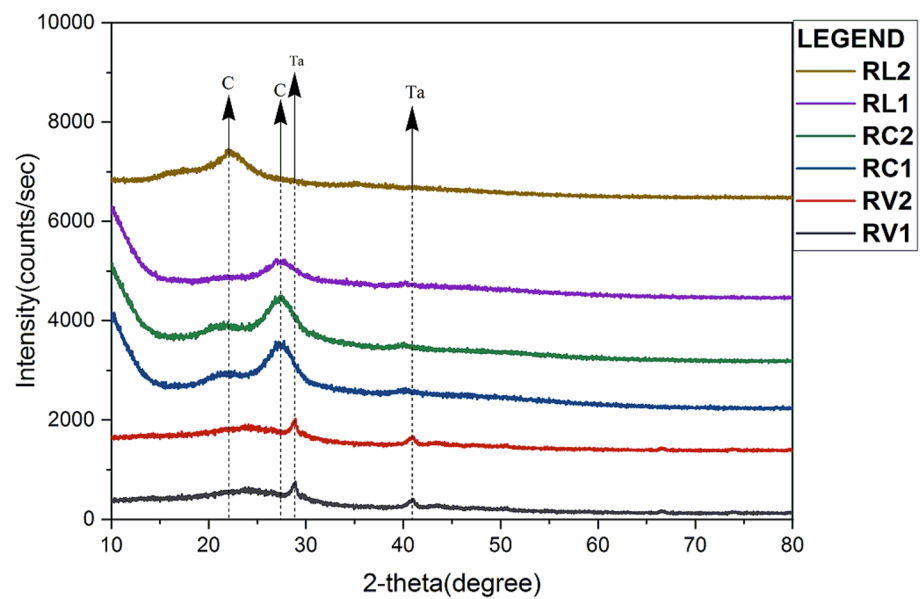
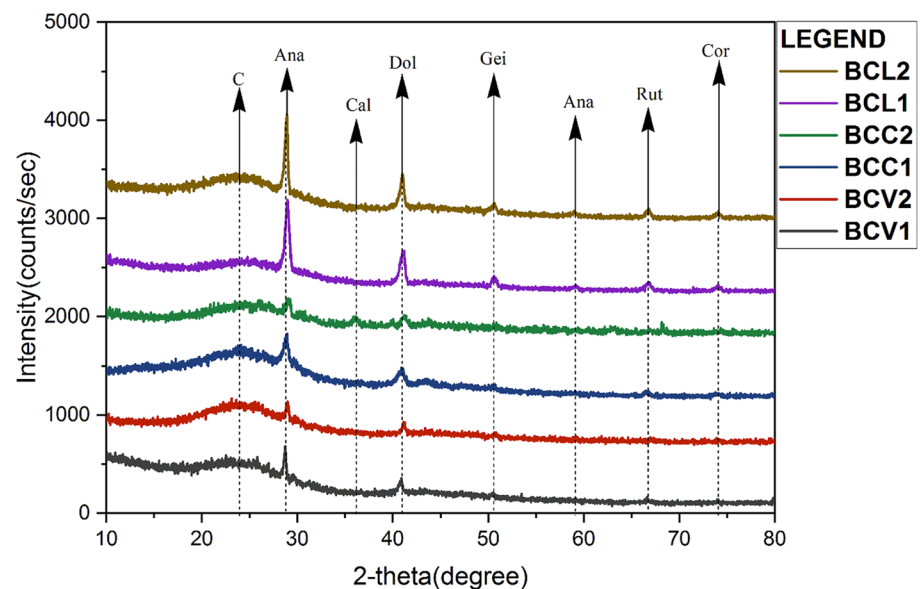


Fig.5 X-ray diffraction patterns of biochars from non-phytoremediation and phytoremediation biomasses. BCL1: *Chrysopogon zizanioides* non-phytoremediation biochar, BCL2: *Chrysopogon zizanioides* phytoremediation biochar, BCC1: *Cymbopogon nardus* non-phytoremediation biochar, BCC2: *Cymbopogon nardus* phytoremediation biochar, BCL1: *Cymbopogon citratus* non-phytoremediation biochar and BCL2: *Cymbopogon citratus* phytoremediation biochar. C: amorphous carbon, Ana: anatase, Cal: calcite, Dol: dolomite, Gei: Geikielite, Rut: rutile and Cor: corronidium



difference in the raw biomass which is a function of the genetic variability between species and the quantity of different elements including HM in growing media. *Cymbopogon citratus* biochars produced from phytoremediation and non-phytoremediation biomasses both contained an almost comparable proportion of anatase (2θ value of 32.8°) as the dominant mineral phase followed by dolomite, geikielite, rutile, corronidium, amorphous carbon, and anatase (2θ value of 62.1°). Anatase was observed to be the dominant mineral in *Cymbopogon nardus* non-phytoremediation biochar followed by amorphous carbon, dolomite, geikielite, and rutile, whereas the counterpart was dominated by anatase followed by amorphous carbon, dolomite, and geikielite, respectively.

Hän et al. [3] attributed the weakening of the x-ray diffraction peaks of phytoremediation biochars to heavy metal carbon structure disordering and constricted graphitization of biochar while sharp peaks are associated with the presence of inorganic constituents [3, 50].

Scanning Electron Microscope Analysis of Ordinary biochars

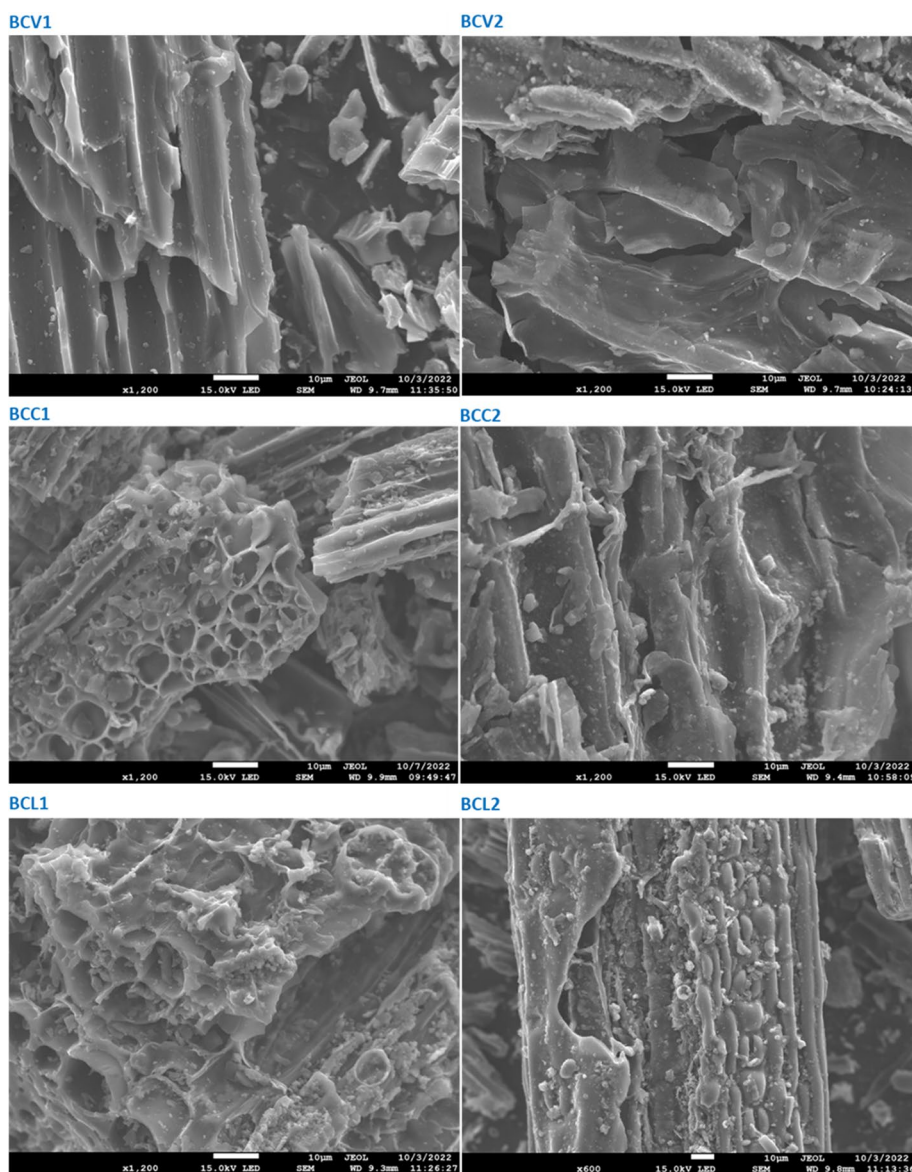
Biochars displayed rough and undefined surfaces with cavities. Biochars derived from non-phytoremediation biomasses had more porous surface structures when compared to phytoremediation biochars as shown in Fig. 6. Pore development

in biochar surfaces is attributed to the thermal degradation of polymer chains of cellulose during the pyrolysis of raw biomasses [51]. With respect to biochars produced from non-phytoremediation biomasses, biochar from *Cymbopogon nardus* exhibited more pores followed by *Cymbopogon citratus* and *Chrysopogon zizanioides*, while for biochars derived from phytoremediation biomasses, *Cymbopogon citratus* had more porous surfaces compared to other grass types. The observation of relatively few pores on the surfaces of phytoremediation biochars suggests that biochar's inherent HM do not favor the formation of micropores within the biochar matrix. The filling of cavities on biochar surfaces is attributed to inorganic substances or minerals detected by XRD analysis [52, 53].

Relationship Between Biochar Chemical Properties and Principal Components (PCs)

PC1 had a very strong negative correlation with biochar pH and EC, as well as ash content, but it had a strong positive correlation with Al, Fe, and Ni while Pb showed a very weak positive correlation with PC1, and Zn had a moderate positive correlation with PC1. Fixed carbon content and volatile matter content displayed a strong positive correlation with PC1. PC2 exhibited a very weak inverse relationship with Al, Cr, Cu, Fe, Ni, and Pb while biochar EC had a very weak positive correlation with PC2. Zn, ash, and volatile matter contents displayed a weak negative relationship with PC2. Biochar pH and fixed carbon contents indicated a weak positive correlation with PC2. These results support that the functional characteristics

Fig.6 Surface morphologies of ordinary biochars from non-phytoremediation and phytoremediation biomasses. BCV1: *Chrysopogon zizanioides* non-phytoremediation biochar, BCV2: *Chrysopogon zizanioides* phytoremediation biochar, BCC1: *Cymbopogon nardus* non-phytoremediation biochar, BCC2: *Cymbopogon nardus* phytoremediation biochar, BCL1: *Cymbopogon citratus* non-phytoremediation biochar and BCL2: *Cymbopogon citratus* phytoremediation biochar



of biochar is influenced by HM in phytoremediation biomasses.

Conclusion

This paper reports that biochar from phytoremediation biomasses contained higher Al, Cu, Ni, Cr, Fe and Zn concentrations regardless of the grass species. Biochars from phytoremediation biomasses displayed a higher biochar yield and ash content, volatile matter content but had low fixed carbon, pH, and electrical conductivity compared to the biochar from non-phytoremediation biomass. FTIR analysis of biomasses showed that the peak intensities of C–H stretching at 2845 cm⁻¹ and 2918 cm⁻¹ of the raw biomasses decreased from non-phytoremediation biomasses to phytoremediation biomasses. Amongst grass species, the intensity of these functional groups descended as follows: *Cymbopogon citratus* > *Chrysopogon zizanioides* > *Cymbopogon nardus*, respectively. FTIR data of biochars which were subjected to principal component analysis resulted in extraction of 2 principal components (PC) which contributed approximately 57.14% and 41.77% of data variance, corresponding to PC1 and PC2, respectively. The biplot was able to discriminate biochar samples based on both types of grass species and the source of biomass. The biplot indicated an increase in identified functional groups from non-phytoremediation biochars to phytoremediation biochars except for *Cymbopogon citratus*. Biochars from *Chrysopogon zizanioides* phytoremediation biochars showed low intensities of anatase and dolomite peaks. Overall, the results of the study have shown the unique characteristics of biochar from phytoremediation biomasses, and also that biochar's characteristics depends on the chemical composition of the raw biomass. The pyrolysis of the phytoremediation biomass will produce biochar as an alternative option for the utilization of biomass derived from phytoremediation in a contaminated environment. The biochar produced could be used for several applications in agriculture and for the environment as a soil conditioner, or for the adsorbent of contaminants in wastewater. However, studies should be conducted with respect to the (1) optimization of the pyrolysis condition of phytoremediation biomasses depending on the type of plant material (species), (2) the kind and concentration of heavy metal contaminants present in the raw biomass and

their relationships to biochar's properties; and (3) to continuously identify and develop potential uses for biochar products from phytoremediation biomasses.

Appendices

Appendix I List of abbreviations used in the current study

Anova	Analysis of variance
BAF	Bioaccumulation factor
BC	Biochar
BCC1	<i>Cymbopogon nardus</i> non-phytoremediation biochar
BCC2	<i>Cymbopogon nardus</i> phytoremediation biochar
BCL	Bamangwato Concessions Limited
BCL1	<i>Cymbopogon citratus</i> non-phytoremediation biochar
BCL2	<i>Cymbopogon citratus</i> phytoremediation biochar
BCV1	<i>Chrysopogon zizanioides</i> non-phytoremediation biochar
BCV2	<i>Chrysopogon zizanioides</i> phytoremediation biochar
CDF	Cation diffusion facilitator
EC	Electrical conductivity
EDX	Energy dispersive X-ray
FC	Fixed carbon
FTIR	Fourier transformer infrared
IBI	International biochar initiative
ICP-OES	Inductively coupled plasma-optical emission spectroscopy
Nramp	Natural resistance -associated macrophage protein
PC	Principal component
PCA	Principal component analysis
PVC	Polyvinylchloride
SB	Source of biomass
TG	Type of grass
VM	Volatile matter
ZIP	Natural resistance -associated macrophage protein

Appendix II EDX analysis of biochar derived from phytoremediation and non-phytoremediation biomasses

Sample names	Atomic (%)														
	C K	O K	Mg K	Al K	Si K	P K	S K	Cl K	K K	Ca K	Mn K	Fe K	Cu K	Zn K	Mo K
BCV1	81.00	12.56	0.50	ND	3.33	ND	0.33	0.33	1.41	0.27	ND	0.06	0.15	0.08	ND
BCV2	78.48	15.06	0.33	0.51	2.60	0.05	0.27	0.23	0.98	0.47	ND	0.47	0.21	0.21	0.12
BCC1	76.23	15.76	0.20	0.17	5.48	ND	0.24	0.26	0.65	0.53	0.04	0.2	0.23	ND	ND
BCC2	79.24	12.89	0.31	0.13	5.19	0.06	0.08	0.60	0.24	0.35	ND	0.12	0.27	0.42	0.11
BCL1	77.31	13.13	0.55	ND	3.26	0.21	ND	0.72	2.67	1.33	0.06	0.05	0.44	0.22	0.04
BCL2	80.27	12.35	0.27	0.03	3.32	0.15	ND	0.60	1.78	0.79	0.01	0.05	0.28	0.12	ND

BCV1: *Chrysopogon zizanioides* non-phytoremediation biochar, BCV2: *Chrysopogon zizanioides* phytoremediation biochar, BCC1: *Cymbopogon nardus* non-phytoremediation biochar, BCC2: *Cymbopogon nardus* phytoremediation biochar, BCL1: *Cymbopogon citratus* non-phytoremediation biochar, BCL2: *Cymbopogon citratus* phytoremediation biochar and EDX: energy dispersive X-ray; ND: not detected

Author Contributions All authors contributed to sample collection, data generation and analysis, and compilation of the manuscript. All authors revised and approved the final manuscript.

Funding Funding was provided by BIUST (S00357) and DRST (AJCore).

Data Availability No other data associated with this manuscript.

Declarations

Competing interest There is no competing interest declared by the authors.

References

- Lee, J.H.: An overview of phytoremediation as a potentially promising technology for environmental pollution control. *Biotechnol. Bioprocess Eng.* **18**, 431–439 (2013). <https://doi.org/10.1007/s12257-013-0193-8>
- He, J., Strezov, V., Kumar, R., Weldekidan, H., Jahan, S., Dastjerdi, B.H., Zhou, X., Kan, T.: Pyrolysis of heavy metal contaminated *Avicennia marina* biomass from phytoremediation: characterisation of biomass and pyrolysis products. *J. Clean. Prod.* **234**, 1235–1245 (2019). <https://doi.org/10.1016/j.jclepro.2019.06.285>
- Han, Z., Guo, Z., Zhang, Y., Xiao, X., Xu, Z., Sun, Y.: Pyrolysis characteristics of biomass impregnated with cadmium, copper and lead: influence and distribution. *Waste Biomass Valoriz.* **9**, 1223–1230 (2018). <https://doi.org/10.1007/s12649-017-0036-5>
- Yuan, X., Xiong, T., Yao, S., Liu, C., Yin, Y., Li, H., Li, N.: A real filed phytoremediation of multi-metals contaminated soils by selected hybrid sweet sorghum with high biomass and high accumulation ability. *Chemosphere* **237**, 124536 (2019). <https://doi.org/10.1016/j.chemosphere.2019.124536>
- Waliszewska, B., Mleczek, M., Zborowska, M., Goliński, P., Rutkowski, P., Szentner, K.: Changes in the chemical composition and the structure of cellulose and lignin in elm wood exposed to various forms of arsenic. *Cellulose* **26**, 6303–6315 (2019). <https://doi.org/10.1007/s10570-019-02511-z>
- Liu, Q., Luo, L., Zheng, L.: Lignins: biosynthesis and biological functions in plants. *Int. J. Mol. Sci.* (2018). <https://doi.org/10.3390/ijms19020335>
- Dražić, G., Milovanović, J., Stefanović, S., Petrić, I.: Potential of *Miscanthus × Giganteus* for heavy metals removing from industrial deposal. *Acta Reg. Environ.* **14**, 56–58 (2017). <https://doi.org/10.1515/aree-2017-0009>
- Vocciante, M., Caretta, A., Bua, L., Bagatin, R., Franchi, E., Petruzzelli, G., Ferro, S.: Enhancements in phytoremediation technology: Environmental assessment including different options of biomass disposal and comparison with a consolidated approach. *J. Environ. Manag.* **237**, 560–568 (2019). <https://doi.org/10.1016/j.jenvman.2019.02.104>
- Inyang, M.I., Gao, B., Yao, Y., Xue, Y., Zimmerman, A., Mosa, A., Pullammanappallil, P., Ok, Y.S., Cao, X.: A review of biochar as a low-cost adsorbent for aqueous heavy metal removal. *Crit. Rev. Environ. Sci. Technol.* **46**, 406–433 (2016). <https://doi.org/10.1080/10643389.2015.1096880>
- Moreira, R., dos Reis Orsini, R., Vaz, J.M., Pentead, J.C., Spinacé, E.V.: Production of biochar, bio-oil and synthesis gas from cashew nut shell by slow pyrolysis. *Waste Biomass Valoriz.* **8**, 217–224 (2017). <https://doi.org/10.1007/s12649-016-9569-2>
- Chai, Y., Chen, A., Bai, M., Peng, L., Shao, J., Yuan, J., Shang, C., Zhang, J., Huang, H., Peng, C.: Valorization of heavy metal contaminated biomass: recycling and expanding to functional materials. *J. Clean. Prod.* **366**, 132771 (2022). <https://doi.org/10.1016/j.jclepro.2022.132771>
- Pandey, D., Daverey, A., Arunachalam, K.: Biochar: production, properties and emerging role as a support for enzyme immobilization. *J. Clean. Prod.* **255**, 120267 (2020). <https://doi.org/10.1016/j.jclepro.2020.120267>
- Touray, N., Tsai, W.T., Li, M.H.: Effect of holding time during pyrolysis on thermochemical and physical properties of biochars derived from goat manure. *Waste Biomass Valoriz.* **5**, 1029–1033 (2014). <https://doi.org/10.1007/s12649-014-9315-6>
- Lievens, C., Yperman, J., Vangronsveld, J., Carleer, R.: Study of the potential valorisation of heavy metal contaminated biomass via phytoremediation by fast pyrolysis: part I. Influence of temperature, biomass species and solid heat carrier on the behaviour of heavy metals. *Fuel* **87**, 1894–1905 (2008). <https://doi.org/10.1016/j.fuel.2007.10.021>
- Zeng, K., Li, R., Minh, D.P., Weiss-Hortala, E., Nzihou, A., Zhong, D., Flamant, G.: Characterization of char generated from

- solar pyrolysis of heavy metal contaminated biomass. *Energy* **206**, 118128 (2020). <https://doi.org/10.1016/j.energy.2020.118128>
16. Zeng, K., Li, R., Minh, D.P., Weiss-Hortala, E., Nzihou, A., He, X., Flamant, G.: Solar pyrolysis of heavy metal contaminated biomass for gas fuel production. *Energy* (2019). <https://doi.org/10.1016/j.energy.2019.116016>
 17. Ultra, V.U.: Fly ash and compost amendments and mycorrhizal inoculation enhanced the survival and growth of delonix regia in cu-ni mine tailings. *Philipp. J. Sci.* **149**, 479–489 (2020)
 18. Ultra, V.U., Ngwako, K.M., Eliason, P.: Physiological responses, growth, and heavy metal accumulation of citronella (*Cymbopogon nardus* Rendle.) in Cu-Ni mine tailings as affected by soil amendments. *Philipp. J. Sci.* **151**, 1241–1254 (2022). <https://doi.org/10.56899/151.03.36>
 19. Taupedi, S.B., Ultra, V.U.: Morupule fly ash as amendments in agricultural soil in Central Botswana. *Environ. Technol. Innov.* **28**, 102695 (2022). <https://doi.org/10.1016/j.eti.2022.102695>
 20. He, J., Strezov, V., Kan, T., Weldekidan, H., Kumar, R.: Slow pyrolysis of metal (loid) rich biomass from phytoextraction: characterisation of biomass, biochar and bio-oil. *Energy Procedia*. **160**, 178–185 (2019). <https://doi.org/10.1016/j.egypro.2019.02.134>
 21. Mirecki, N., Agič, R., Šunić, L., Milenković, L., Ilić, Z.S.: Transfer factor as indicator. *Fresenius Environ. Bull.* **24**, 4212 (2015)
 22. Liu, T., Liu, B., Zhang, W.: Nutrients and heavy metals in biochar produced by sewage sludge pyrolysis: its application in soil amendment. *Polish J. Environ. Stud.* **23**, 271–275 (2014)
 23. Tomczyk, A., Sokołowska, Z., Boguta, P.: Biochar physicochemical properties: pyrolysis temperature and feedstock kind effects. *Rev. Environ. Sci. Biotechnol.* **19**, 191–215 (2020). <https://doi.org/10.1007/s11157-020-09523-3>
 24. Basant, N., Singh, J., Kumari, B., Sinam, G., Gautam, A., Singh, G., et al.: Nickel and cadmium phytoextraction efficiencies of vetiver and lemongrass grown on Ni–Cd battery waste contaminated soil: a comparative study of linear and nonlinear models. *J. Environ. Manag.* **295**, 113144 (2021). <https://doi.org/10.1016/j.jenvm.2021.113144>
 25. Chukwuma, O.B., Rafatullah, M., Tajarudin, H.A., Ismail, N.: Lignocellulolytic enzymes in biotechnological and industrial processes: a review. *Sustain.* **12**, 1–31 (2020). <https://doi.org/10.3390/su12187282>
 26. Wang, X., Li, C., Li, Z., Yu, G., Wang, Y.: Effect of pyrolysis temperature on characteristics, chemical speciation and risk evaluation of heavy metals in biochar derived from textile dyeing sludge. *Ecotoxicol. Environ. Saf.* **168**, 45–52 (2019). <https://doi.org/10.1016/j.ecoenv.2018.10.022>
 27. Saletnik, B., Zagula, G., Bajcar, M., Tarapatsky, M., Bobula, G., Puchalski, C.: Biochar as a multifunctional component of the environment—a review. *Appl. Sci.* (2019). <https://doi.org/10.3390/app9061139>
 28. He, J., Kumar, R., Kan, T., Strezov, V.: A state-of-the-art review of the fate of heavy metals and product properties from pyrolysis of heavy-metal(loid)-enriched biomass harvested from phytoextraction. *Environ. Prog. Sustain. Energy.* **42**, 1–17 (2023). <https://doi.org/10.1002/ep.13979>
 29. Jung, S.H., Kang, B.S., Kim, J.S.: Production of bio-oil from rice straw and bamboo sawdust under various reaction conditions in a fast pyrolysis plant equipped with a fluidized bed and a char separation system. *J. Anal. Appl. Pyrolysis.* **82**, 240–247 (2008). <https://doi.org/10.1016/j.jaap.2008.04.001>
 30. Domingues, R.R., Trugilho, P.F., Silva, C.A., De Melo, I.C.N.A., Melo, L.C.A., Magriotis, Z.M., Sánchez-Monedero, M.A.: Properties of biochar derived from wood and high-nutrient biomasses with the aim of agronomic and environmental benefits. *PLoS ONE* **12**, 1–19 (2017). <https://doi.org/10.1371/journal.pone.0176884>
 31. Wang, S., Zou, C., Lou, C., Yang, H., Mei, M., Jing, H., Cheng, S.: Effects of hemicellulose, cellulose and lignin on the ignition behaviors of biomass in a drop tube furnace. *Bioresour. Technol.* **310**, 123456 (2020). <https://doi.org/10.1016/j.biortech.2020.123456>
 32. Liu, A., Chen, J., Lu, X., Li, D., Xu, W.: Influence of components interaction on pyrolysis and explosion of biomass dust. *Process Saf. Environ. Prot.* **154**, 384–392 (2021). <https://doi.org/10.1016/j.psep.2021.08.032>
 33. Du, J., Zhang, L., Liu, T., Xiao, R., Li, R., Guo, D., Qiu, L., Yang, X., Zhang, Z.: Thermal conversion of a promising phytoremediation plant (*Symphytum officinale* L.) into biochar: dynamic of potentially toxic elements and environmental acceptability assessment of the biochar. *Bioresour. Technol.* **274**, 73–82 (2019). <https://doi.org/10.1016/j.biortech.2018.11.077>
 34. Zeng, Z., Zhang, S.D., Li, T.Q., Zhao, F.L., He, Z.L., Zhao, H.P., Yang, X.E., Wang, H.L., Zhao, J., Rafiq, M.T.: Sorption of ammonium and phosphate from aqueous solution by biochar derived from phytoremediation plants. *J. Zhejiang Univ. Sci. B.* **14**, 1152–1161 (2013). <https://doi.org/10.1631/jzus.B1300102>
 35. Rehrah, D., Reddy, M.R., Novak, J.M., Bansode, R.R., Schimmel, K.A., Yu, J., Watts, D.W., Ahmedna, M.: Production and characterization of biochars from agricultural by-products for use in soil quality enhancement. *J. Anal. Appl. Pyrolysis.* **108**, 301–309 (2014). <https://doi.org/10.1016/j.jaap.2014.03.008>
 36. Sun, J., He, F., Pan, Y., Zhang, Z.: Effects of pyrolysis temperature and residence time on physicochemical properties of different biochar types. *Acta Agric. Scand. Sect. B* **67**, 12–22 (2017). <https://doi.org/10.1080/09064710.2016.1214745>
 37. De Conto, D., Silvestre, W.P., Baldasso, C., Godinho, M.: Performance of rotary kiln reactor for the elephant grass pyrolysis. *Bioresour. Technol.* **218**, 153–160 (2016). <https://doi.org/10.1016/j.biortech.2016.06.082>
 38. Amari, T., Ghnaya, T., Abdely, C.: Nickel, cadmium and lead phytotoxicity and potential of halophytic plants in heavy metal extraction. *South Afr. J. Bot.* **111**, 99–110 (2017). <https://doi.org/10.1016/j.sajb.2017.03.011>
 39. Lu, T., Yuan, H., Wang, Y., Huang, H., Chen, Y.: Characteristic of heavy metals in biochar derived from sewage sludge. *J. Mater. Cycles Waste Manag.* **18**, 725–733 (2016). <https://doi.org/10.1007/s10163-015-0366-y>
 40. Boeriu, C.G., Bravo, D., Gosselink, R.J.A., Van Dam, J.E.G.: Characterisation of structure-dependent functional properties of lignin with infrared spectroscopy. *Ind. Crops Prod.* **20**, 205–218 (2004). <https://doi.org/10.1016/j.indcrop.2004.04.022>
 41. Wang, X., Ren, H.: Comparative study of the photo-discoloration of moso bamboo (*Phyllostachys pubescens* Mazel) and two wood species. *Appl. Surf. Sci.* **254**, 7029–7034 (2008). <https://doi.org/10.1016/j.apsusc.2008.05.121>
 42. Liu, J., Zhang, Q.H., Ma, F., Zhang, S.F., Zhou, Q., Huang, A.M.: Three-step identification of infrared spectra of similar tree species to *Pterocarpus santalinus* covered with beeswax. *J. Mol. Struct.* **1218**, 128484 (2020). <https://doi.org/10.1016/j.molstruc.2020.128484>
 43. Jaruwat, D., Udomsap, P., Chollacoop, N., Fuji, M., Eiad-Ua, A.: Effects of hydrothermal temperature and time of hydrochar from Cattail leaves. *AIP Conf. Proc.* (2018). <https://doi.org/10.1063/1.5053192>
 44. Md Salim, R., Asik, J., Sarjadi, M.S.: Chemical functional groups of extractives, cellulose and lignin extracted from native *Leucaena leucocephala* bark. *Wood Sci. Technol.* **55**, 295–313 (2021). <https://doi.org/10.1007/s00226-020-01258-2>
 45. Oves, M., Khan, M.S., Zaidi, A.: Biosorption of heavy metals by *Bacillus thuringiensis* strain OSM29 originating from industrial effluent contaminated north Indian soil. *Saudi J. Biol. Sci.* **20**, 121–129 (2013). <https://doi.org/10.1016/j.sjbs.2012.11.006>

46. Barrera-zapata, R.: Morphological and physicochemical characterization of biochar produced by gasification of selected forestry species. *Caracterización morfológica y físico-química de biocarbonos producidos*. *Revista Facultad de Ingeniería* **26**, 123–130 (2017)
47. Wang, N., Chen, Q., Zhang, C., Dong, Z., Xu, Q.: Improvement in the physicochemical characteristics of biochar derived from solid digestate of food waste with different moisture contents. *Sci. Total Environ.* **819**, 153100 (2022). <https://doi.org/10.1016/j.scitotenv.2022.153100>
48. All, U.T.C.: Plant genotype differences in the uptake, translocation, accumulation, and use of mineral elements required for plant growth. *Plant Soil* **72**, 175–196 (2017)
49. Bilba, K., Ouensanga, A.: Fourier transform infrared spectroscopic study of thermal degradation of sugar cane bagasse. *J. Anal. Appl. Pyrolysis.* **38**, 61–73 (1996). [https://doi.org/10.1016/S0165-2370\(96\)00952-7](https://doi.org/10.1016/S0165-2370(96)00952-7)
50. Colombo, C., Palumbo, G., He, J.Z., Pinton, R., Cesco, S.: Review on iron availability in soil: interaction of Fe minerals, plants, and microbes. *J. Soils Sediments.* **14**, 538–548 (2014). <https://doi.org/10.1007/s11368-013-0814-z>
51. Al-Jumaily, M.M., Al-Hamandi, H.M., Al-Obaidi, M.A., Al-Zidan, R.R.: Quantity-intensity ratio of potassium in gypsiferous soils in Iraq. *Pesqui. Agropecu. Trop.* (2022). <https://doi.org/10.1590/1983-40632022v5271620>
52. Kim, K.H., Kim, J.Y., Cho, T.S., Choi, J.W.: Influence of pyrolysis temperature on physicochemical properties of biochar obtained from the fast pyrolysis of pitch pine (*Pinus rigida*). *Bioresour. Technol.* **118**, 158–162 (2012). <https://doi.org/10.1016/j.biortech.2012.04.094>
53. Tushar, M.S.H.K., Mahinpey, N., Khan, A., Ibrahim, H., Kumar, P., Idem, R.: Production, characterization and reactivity studies of chars produced by the isothermal pyrolysis of flax straw. *Biomass Bioenergy.* **37**, 97–105 (2012). <https://doi.org/10.1016/j.biombioe.2011.12.027>

Publisher's Note Springer Nature remains neutral with regard to jurisdictional claims in published maps and institutional affiliations.

Springer Nature or its licensor (e.g. a society or other partner) holds exclusive rights to this article under a publishing agreement with the author(s) or other rightsholder(s); author self-archiving of the accepted manuscript version of this article is solely governed by the terms of such publishing agreement and applicable law.